UDC 617.581/.582-089.843:616.71:615.461]-091.8-092.9 https://doi.org/10.26641/2307-0404.2025.4.348747

O.O. Bondarenko [*],
A.E. Lievykh,
N.S. Bondarenko,
A.G. Bozhko,
O.Ye. Loskutov,
I.S. Shponka

EXPRESSION OF VEGF, BMP-2, AND THE OPG/RANK AXIS AS INDICATORS OF OSSEOINTEGRATION: A COMPARATIVE CLINICAL AND EXPERIMENTAL STUDY OF TITANIUM IMPLANTS WITH FUNCTIONAL PROTECTIVE COATINGS

Dnipro State Medical University
Volodymyra Vernadskoho str., 9, Dnipro, 49044, Ukraine
Дніпровський державний медичний університет
вул. Володимира Вернадського, 9, Дніпро, 49044, Україна
[*]*e-mail: bondarenko.olexandr@dmu.edu.ua*

Цитування: Медичні перспективи. 2025. Т. 30, № 4. С. 12-23
Cited: Medicni perspektivi. 2025;30(4):12-23

Key words: *osteoinduction, osteoconduction, osseointegration, titanium implant, alumina, translational study, vascular-endothelial growth factor, receptor of vascular-endothelial growth factor, bone morphogenetic protein 2, osteoprotegerin/receptor activator of nuclear factor κB axis, enzyme-linked immunosorbent assay, bone remodeling, immunohistochemistry*
Ключові слова: *остеоіндукція, остеокондукція, остеоінтеграція, титановий імплантат, оксид алюмінію, трансляційне дослідження, фактор росту ендотелію судин, рецептор фактора росту ендотелію судин, кістковий морфогенетичний протеїн 2, вісь остеопротегерин/рецептор-активатор ядерного фактора κВ, імуноферментний аналіз, ремоделювання кісток, імуногістохімія*

Abstract. Expression of VEGF, BMP-2, and the OPG/RANK axis as indicators of osseointegration: a comparative clinical and experimental study of titanium implants with functional protective coatings. Bondarenko O.O., Lievykh A.E., Bondarenko N.S., Bozhko A.G., Loskutov O.Ye., Shponka I.S. *The objective of the present study was to validate key molecular markers of bone tissue repair as indicators of osseointegration on systemic and local levels, and evaluate their translational parallelism. This was achieved by comparing the configurational consistency of expression profiles between an experimental rat model and a pilot clinical investigation in human patients to synchronize systemic and local molecular responses. The hypothesis was that alumina-coated titanium implants would exhibit faster dynamics of angiogenic and osteogenic biomarkers, indicating accelerated osteoinduction, osteoconduction, and osseointegration compared with uncoated titanium. The pilot clinical study comprised the patients after total hip arthroplasty (n=6): three with uncoated titanium implants and three with alumina ceramics. Serum samples were collected from these patients in one and six months post-surgery. The experimental rat model comprised 160 Wistar females implanted with modified intrafemoral implants (seven surface types, including uncoated and alumina-coated titanium), with serum and peri-implant tissue samples collected in one, two, four, and eight weeks. Serum levels of vascular endothelial growth factor, bone morphogenetic protein 2, and osteoprotegerin were determined by enzyme-linked immunosorbent assay, while the corresponding local expression of vascular endothelial growth factor receptor, bone morphogenetic protein 2, and receptor activator of nuclear factor kappa-B was assessed by immunohistochemistry. The results demonstrated that alumina-coated implants induced an accelerated and synchronized molecular cascade in the rat model, which was qualitatively replicated in the clinical cohort. The systemic vascular endothelial growth factor peak manifested early, at one week in rats and one month in humans, and exhibited a strong parallelism with local microvessel density in the animal model, confirming rapid angiogenic activation. In both species, the expression of bone morphogenetic protein 2 increased earlier and to a greater extent in the alumina-coated groups, indicating more rapid osteoinduction. Local receptor activator of nuclear factor kappa-B activity demonstrated an early rise and a four-week peak in the groups with coated implants, consistent with controlled and timely bone remodelling. The study indicates that alumina coatings promote accelerated osseointegration by advancing the time course of healing, a conclusion supported by the observed translational parallelism of the investigated markers.*

Реферат. Експресія VEGF, BMP-2 та вісі OPG/RANK як індикатори остеоінтеграції: порівняльне клініко-експериментальне дослідження титанових імплантатів з функціональними захисними покриттями. Бондаренко О.О., Лєвих А.Е., Бондаренко Н.С., Божко А.Г., Лоскутов О.Е., Шпонька І.С. *Метою цього дослідження було підтвердження ключових молекулярних маркерів відновлення кісткової тканини як індикаторів остеоінтеграції на системному та місцевому рівнях, а також оцінювання їх трансляційного паралелізму. Це було*

досягнуто шляхом порівняння конфігураційної узгодженості профілів експресії між експериментальною моделлю на щурах та пілотним клінічним дослідженням на пацієнтах з метою перевірки узгодженості системних та місцевих молекулярних реакцій. Гіпотеза полягала в тому, що титанові імплантати з покриттям з оксиду алюмінію демонструватимуть швидшу динаміку ангіогенних та остеогенних біомаркерів, що вказує на прискорену остеоіндукцію, остеокондукцію та остеоінтеграцію порівняно з непокритим титаном. Пілотне клінічне дослідження охоплювало пацієнтів після тотального ендопротезування кульшового суглоба (n=6): трьох – з непокритими титановими імплантатами та трьох – з керамічними імплантатами з оксиду алюмінію. Зразки сироватки крові були зібрані в цих пацієнтів через один і шість місяців після операції. Експериментальна модель на щурах складалася зі 160 самок породи Вістар, яким були введені модифіковані внутрішньостегнові імплантати (сім типів поверхні, включаючи непокритий і покритий оксидом алюмінію титан), зразки сироватки крові та тканин навколо імплантата були зібрані через один, два, чотири та вісім тижнів. Рівні сироваткового фактора росту ендотелію судин, кісткового морфогенетичного білка 2 та остеопротегерину визначали за допомогою імуноферментного аналізу, а відповідну локальну експресію рецептора фактора росту ендотелію судин, кісткового морфогенетичного білка 2 та активатора рецептора ядерного фактора каппа-В оцінювали за допомогою імуногістохімії. Результати продемонстрували, що імплантати з покриттям з оксиду алюмінію індукували прискорену та синхронізовану каскадну реакцію біомолекул у моделі на щурах, що було якісно відтворено в клінічній когорті. Пік експресії системного фактора росту ендотелію судин проявився на ранніх етапах, через тиждень у щурів і через місяць у людей та виявляв сильний паралелізм з локальною щільністю мікросудин у моделі на тваринах, що підтверджує швидку ангіогенну активацію. В обох видах експресія кісткового морфогенетичного білка 2 збільшилася раніше і більшою мірою в групах з покриттям з оксиду алюмінію, що вказує на більш швидку остеоіндукцію. Місцевий активатор рецептора ядерного фактора каппа-В продемонстрував раннє підвищення і чотиритижневий пік у групах з покритими імплантатами, що відповідає контрольованому і своєчасному ремоделюванню кісткової тканини. Дослідження показує, що алюмінієві покриття сприяють прискоренню остеоінтеграції, скорочуючи час загоєння, і цей висновок підтверджується спостережуваним трансляційним паралелізмом досліджуваних маркерів.

The successful osseointegration of titanium implants is contingent upon a finely regulated balance between bone resorption and formation at the bone-implant interface. This dynamic process involves a coordinated sequence of cellular events, including inflammation, osteoclastic bone resorption, and subsequent osteoblastic bone formation. The quality and speed of integration at these stages is determined by critical molecular regulators, including vascular endothelial growth factor (VEGF), bone morphogenetic protein 2 (BMP-2), and the osteoprotegerin (OPG)/receptor activator of nuclear factor κB (RANK)/RANK ligand (RANKL) signaling axis [1]. It is imperative to comprehend the expression patterns in order to gain profound insights into the biological performance of implant surface coatings. VEGF is one of the earliest signaling molecules that is upregulated after implantation and serves as a potent mediator of angiogenesis [2, 3, 4]. By promoting vascular ingrowth into the developing peri-implant tissue, VEGF ensures adequate oxygen and nutrient delivery, facilitating the recruitment and differentiation of osteogenic cells. The degree of VEGF expression has been consistently correlated with new bone formation and implant stability, suggesting its potential as an early biomarker of successful osseointegration [5]. BMP-2, a pivotal member of the transforming growth factor-β (TGF-β) superfamily, is an indispensable osteoinductive factor that stimulates mesenchymal stem cell differentiation into osteoblasts and enhances extracellular matrix mineralization [6, 7, 8]. Its sustained expression during the remodeling phase has been demonstrated to support the maturation of newly formed bone and the successful integration of the implant [9, 10, 11]. Materials that promote early and sustained BMP-2 upregulation have been shown to yield superior bone-implant interface and accelerated osseointegration [11,12].

Concurrent with these osteogenic mechanisms, the OPG/RANK/RANKL axis orchestrates bone resorption and remodeling [1]. RANK, expressed on osteoclast precursors, binds to its ligand RANKL, thereby triggering osteoclast differentiation and activation. OPG, a soluble decoy receptor for RANKL, competitively inhibits this interaction. The resulting OPG/RANKL ratio thus reflects the state of bone turnover: a low ratio indicates active early resorption, while a rising ratio marks the transition to equilibrium and mature bone formation, a process essential for long-term implant stability [14].

As demonstrated in previous publications, these molecular markers have been shown to play a pivotal role in the process of bone healing when studied across a range of models [1, 14, 15]. For instance, studies conducted on roughened titanium surfaces have demonstrated that enhanced osseointegration is associated with the transient upregulation of VEGF and BMP-2 expression in vivo, particularly in rodent models [11, 16, 17, 18]. In a similar vein, the local expression ratio of OPG/RANKL has been identified as a reliable predictor of bone stability surrounding dental implants [1, 14, 15]. However, a direct comparative investigation that links the molecular response (VEGF, BMP-2, and the OPG/RANK axis) to a specific, emerging coating

technology (alumina-based) across both a preclinical model (rat) and the clinical setting (human) is notably scarce. The absence of translational data indicates a significant knowledge deficit, hindering the ability to reliably predict clinical outcomes based solely on experimental findings.

The primary objective of the present study is to establish the translational parallelism of key systemic molecular markers (VEGF, BMP-2, and OPG) as indicators of osseointegration by correlating expression profiles in a rodent model and pilot clinical study of human patients. Concurrently, the objective of the study was to make a comparison between the temporal dynamics of these systemic markers and the local expression of their functional equivalents, receptors, or antagonists (VEGFR, BMP-2, RANK) in the peri-implant bone tissue of the rat model, providing a critical mechanistic evidence of the coating's osteoconductive potential. It is hypothesized that alumina-coated titanium implants will demonstrate a molecular pattern indicative of controlled bone turnover and earlier stabilization in comparison with uncoated titanium implants.

MATERIALS AND METHODS OF RESEARCH

Implant materials. The manufacturing process of the implants, along with their physical and chemical properties, has been detailed in previous publications [19, 20]

Animal model. The cylindrical pins were implanted intramedullary into the right femurs of 160 female Wistar rats with average age 17 weeks and weight 250 g. Animals were divided into 7 groups according to implant type (Ti, TS, TSP, TSPC, TSPT, TSPTC and TSPH, Fig. 1) and duration of implant exposure (1, 2, 4, and 8 weeks) with 20 animals in each group. Ti-group (n=20) was implanted with untreated titanium wire, whilst TSPH (n=20) served as a reference group with hydroxyapatite (HAp)-coated group. Additional 20 animals served as a sham-operated negative control group. All surgical and pharmacological interventions, including anesthesia and euthanasia, were described in our previous paper [19, 20]. Rats were maintained on a 12 h light and dark cycle with ad libitum access to water and normal chow diet composed of 10% fat. All animal experiments and procedures mentioned above were performed in compliance with ethical regulations (Law of Ukraine No. 3447-IV and European Directive 2010/63/EU) and the approval of Biomedical Ethics Committee of Dnipro State Medical University (meeting minutes No. 2 dated 26.10.19.).

Pilot clinical investigation. A total of six patients were consecutively enrolled in the pilot clinical investigation at the Department of Trauma Surgery and Orthopaedics, Mechnikov Hospital, Dnipro, between 01.11.2019 and 31.10.2021. The cohort comprised three male and three female patients, with ages ranging from 45 to 63 years. The study was approved by the Biomedical Ethics Committee of Dnipro State Medical University (meeting minutes No. 2, dated 26.10.2019) and conducted in accordance with the Declaration of Helsinki. Written informed consent was obtained from all patients prior to enrolment.

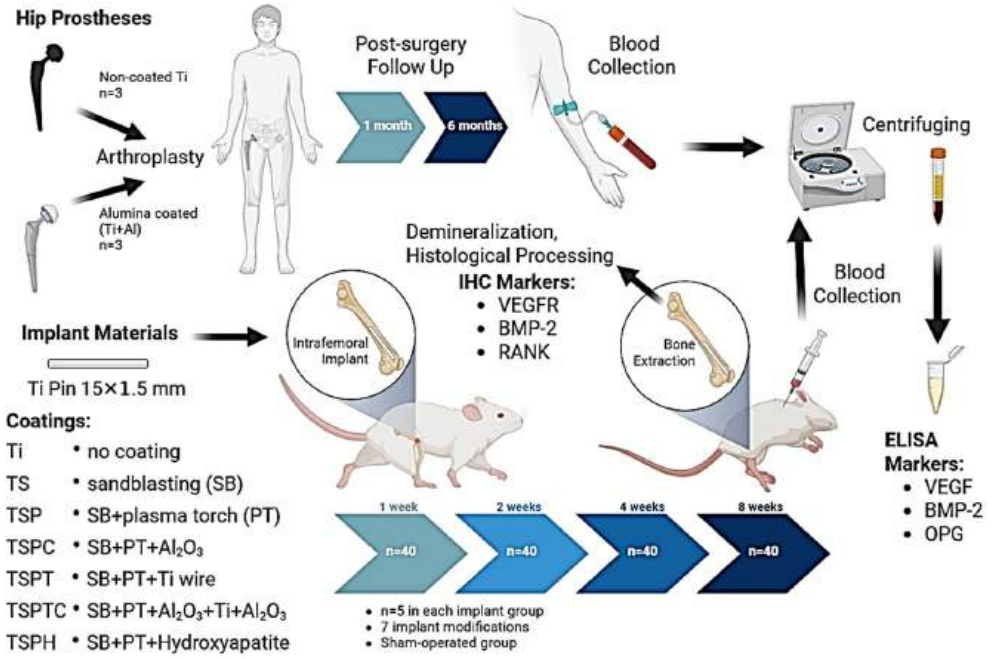

Fig. 1. Study design and experimental workflow illustrating the translational approach of this research

Inclusion criteria stipulated that they must be adults, electively undergoing primary unilateral hip arthroplasty, and capable of providing written informed consent. Exclusion criteria were applied rigorously to minimize confounding variables, encompassing a range of medical conditions, including but not limited to diabetes mellitus, active malignancy, chronic kidney or liver disease, chronic inflammatory or autoimmune disorders, immunosuppressive therapy or chronic corticosteroid use, active infection, prior ipsilateral joint replacement, known coagulopathy, and pregnancy.

Arthroplastic procedures utilize cementless femoral stems and acetabular components manufactured from commercially available titanium alloy (Ti6Al4V). Patients were allocated to one of two groups based on the implant's surface modification, with each group including three patients: (1) Ti group, uncoated titanium alloy implants; (2) Ti+Al group, titanium alloy implants with plasma-sprayed aluminum oxide (Al_2O_3) surface coating.

Postoperative follow-up was performed in 1 and 6 months after surgery. Clinical assessment included wound inspection, pain evaluation, and functional recovery using the Harris Hip Score (HHS). Standard anteroposterior and lateral radiographs were obtained at each visit to assess implant positioning, osseointegration, and signs of early loosening.

ELISA. The serum concentrations of investigated biomarkers were quantified using a sandwich enzyme-linked immunosorbent assay (ELISA). Serum extracts were prepared from patients' blood specimens collected by 1 and 6 months after the hip replacement for each patient; from rat blood specimens collected during the euthanasia procedure from the right ventricle at the corresponding timepoint (1, 2, 4, and 8 weeks). The 4 mL clot activator vacuum tubes (Ayset, Turkey) with collected blood were centrifuged after the blood clot formation for 20 min at 2000 rpm at 4°C and the centrifugates were transferred into chilled tubes and stored at 80°C for further analysis. The following biomarkers were analyzed: rat VEGF, BMP-2, and OPG ELISA kits from Abcam (ab100786, ab213900, and ab255723, Abcam, UK); human VEGF-A, BMP-2, and OPG TNFRSF11b ELISA kits from Sigma (RAB0507, RAB0028, and RAB0484, Sigma, USA). The plates were read at 450 nm and analyzed using a microplate reader (Rayto RT-2100C, China). Investigated concentrations were measured and expressed in pg/ml. All procedures were carried out according to the manufacturers' manuals.

Histological methods. After euthanasia, 1.5 cm fragments of the distal femurs with implants were collected. An electric saw (Dremel-2050, Germany) was used for this purpose, using a diamond-coated disk. The desired bone fragment was carefully separated from the implant and fixed in a 10% formalin buffered in PBS (pH=7.4) for at least 24 hours.

Demineralization was performed in 10% ethylenediamine-tetraacetic acid (EDTA) solution, pH=7.4 at 4°C with agitation during 2 weeks. Demineralized samples were embedded in paraffin and sectioned on rotary microtome HM340E (Thermo Scientific, Germany).

Immunohistochemistry of peri-implant tissues. For the purpose of immunohistochemical (IHC) study, all samples were sectioned of 4 μm thickness, then mounted on Superfrost adhesive slides (Thermo, Germany), deparaffinized with xylene, and rehydrated with downgrading concentrations of ethanol. Endogenous peroxidase activity was blocked using a 3% hydrogen peroxide solution in 70% methanol for 20 minutes at room temperature. The sections were then washed three times in phosphate-buffered saline (PBS) and subjected to heat-induced antigen retrieval (HIAR) by incubation in a water bath with citrate buffer (pH 6.0) for 20 minutes after reaching 98°C. To enhance antigen exposure, the buffer was supplemented with 2 ml of Triton X-100 detergent (Sigma, Germany) per 200 ml, ensuring the symmetrical arrangement of slides within the cuvette [21].

Following three additional PBS washes, the slides were placed on a humidified plate and incubated with a 1% normal goat serum solution in 1% bovine serum albumin (BSA) for 20 minutes to block nonspecific binding. The primary antibodies used were as follows: anti-VEGFR (rabbit polyclonal, 1:800, Thermo Fisher Scientific, USA), anti-BMP-2 (rabbit polyclonal, 1:2000, Thermo Fisher Scientific, USA), and RANK (clone 9A725, 1:500, Thermo Fisher Scientific, USA).

Sections were incubated with primary antibodies overnight at 40°C in a humid chamber. Immunodetection was performed using the Master Polymer Plus Detection System (Master Diagnostica, Spain), followed by visualization with a diaminobenzidine (DAB) chromogen reaction in the presence of hydrogen peroxide and horseradish peroxidase, producing a brown signal at antigen-binding sites [21]. Counterstaining was performed with Gill's hematoxylin for 30 seconds. Finally, sections were dehydrated in graded alcohol, cleared in xylene, and mounted under coverslips using a permanent mounting medium.

Microscopy and histomorphometry. Microscopy was performed using a ZEISS "AxioImager.A2" (Carl Zeiss AR, Germany) light microscope (×10, ×20, ×40 objectives). Digital images and morphometric analysis was carried out with ZEN 2 Blue Edition software (Carl Zeiss AR, Germany).

For the purpose of microvascular density (MVD) assessment, all morphological structures with lumen surrounded by VEGFR-positive endothelial cells

were considered to be blood microvessels. For each section, three separate regions of interest (ROI) with the most prominent neovascularization were selected by visual observation through high-power magnification (×400). In each ROI, measurements were performed counting the vessels number per mm^2. The mean value of these three ROI was considered satisfactory for representation of each specimen. For the morphometric evaluation of BMP-2 and RANK expression in peri-implant bone tissue, BMP-2- or RANK-positive cells were counted in 4 different ROI under the magnification ×400 [4, 17].

Statistics. Statistical analysis was performed using GraphPad Prism version 8.0.2 (263) (GraphPad Software, San Diego, CA, USA) [4,6,17]. For the pilot clinical study, ELISA measurements were expressed as the median ± interquartile range (IQR). Intragroup comparisons (temporal dynamics) were assessed using Wilcoxonmatched-pairs signed-rank test, while intergroup comparisons (implant type) were performed using the Mann-Whitney U-test. In the animal experiment, data distribution was assessed for normality using the Shapiro-Wilk test. ELISA datasets were expressed as the median ± IQR, while morphometrical datasets were consistent with a normal distribution and expressed as the mean ± standard deviation (SD). Comparisons of non-parametric variables (ELISA) were performed using Kruskal-Wallis test followed by Dunn's post hoc test, whereas parametric variables (morphometry) were analyzed using one-way analysis of variance (ANOVA) test. To control alpha-error accumulation across multiple comparisons, the false discovery rate (FDR) was applied using the Benjamini-Hochberg method. Statistical significance was defined as an FDR-adjusted p-value (q-value) <0.05.

Translational Pattern-Matching Analysis. To evaluate translational validity, a pattern-matching analysis was employed based on the design described by Campbell and Yin [22]. In this framework, the dynamics of biomarker serum levels (upregulation, downregulation or stabilization) in rats with alumina coated (TSPC and TSPTC groups) and uncoated (Ti group) Ti implants served as the "expected pattern", which was defined as a specific configuration of variables predicted to occur if the hypothesis of this study is true. Similar values in corresponding groups of patients (Ti+Al and Ti) served as the "observed pattern", which consisted of median serum values obtained from the pilot clinical cohort at biologically equivalent time points, where the first week in rats was paired with the first month in human patients to represent the early (angiogenic) phase, while the eighth week in rats was paired with the sixth month in patients to represent the late (remodeling) phase, in accordance with the reported translational studies [23].

As per Yin's criteria for rigorous testing, the translational hypothesis was considered supported only if the observed pattern matched the expected pattern for the constituent non-equivalent variables in both direction relative to control and temporal order.

RESULTS AND DISCUSSION

ELISA. Serum VEGF levels exhibited time-dependent fluctuations across all investigated and reference groups (Fig. 2A). A week after implantation, the alumina-coated TSPTC group showed concentrations significantly higher than the uncoated titanium ($p<0.0001$) and sham-operated groups ($p<0.05$). TSPT and hydroxyapatite-coated (TSPH) groups also exhibited significantly higher levels compared to the Ti group ($p<0.001$). Surprisingly, TSPC demonstrated lower expression than TSPTC ($p<0.05$), although both groups were implanted with alumina-based implants. In two weeks, the TSPTC group maintained significantly elevated levels compared to both the Ti ($p<0.05$) and sham-operated groups ($p<0.001$). The TSPT group showed the most pronounced response at this time point, significantly exceeding the Ti group ($p<0.001$), sham-operated group ($p<0.0001$), and the TSPH group ($p<0.05$). In four weeks, VEGF values declined across the cohort, and no significant differences were observed between any experimental groups. In eight weeks, VEGF levels in sham-operated group dropped to undetectable levels, whereas other experimental groups did not reveal any significant differences from the Ti or TSPH groups. Generally, VEGF levels demonstrated a downward trend from week 1 to week 8 across all cohorts; however, a statistically significant intra-group decline was confirmed only in TSPTC group (from week 1 to week 4, $p<0.05$; and to week 8, $p<0.05$) and in TSPT group (from week 1 to week 8, $p<0.05$).

Serum BMP-2 levels displayed a delayed onset relative to VEGF (Fig. 2C). In a week after surgery, detectable levels were observed primarily in two animals from the sham-operated group (31 pg/ml). In two weeks, the sham control demonstrated BMP-2 upregulation along with the animals from the TSPH group, while in other experimental groups, BMP-2 was still undetectable. In four weeks, a generalized systemic BMP-2 elevation was observed across all cohorts. The TSPT group exhibited significantly lower levels than the alumina-coated TSPTC group ($p<0.05$) and the TSP group ($p<0.05$). At this time point, no significant differences were detected between the experimental and reference groups (Ti, sham, or TSPH). In eight weeks, the alumina-coated TSPTC group, uncoated Ti group, and TSP group

maintained significantly higher concentrations than the sham control ($p<0.05$), where only one animal remained with detectable BMP-2 levels. Comparing the intragroup dynamics, BMP-2 serum concentrations after the peak in 4 weeks declined across all groups except for the animals with uncoated Ti implants in eight weeks, although no statistical difference was found.

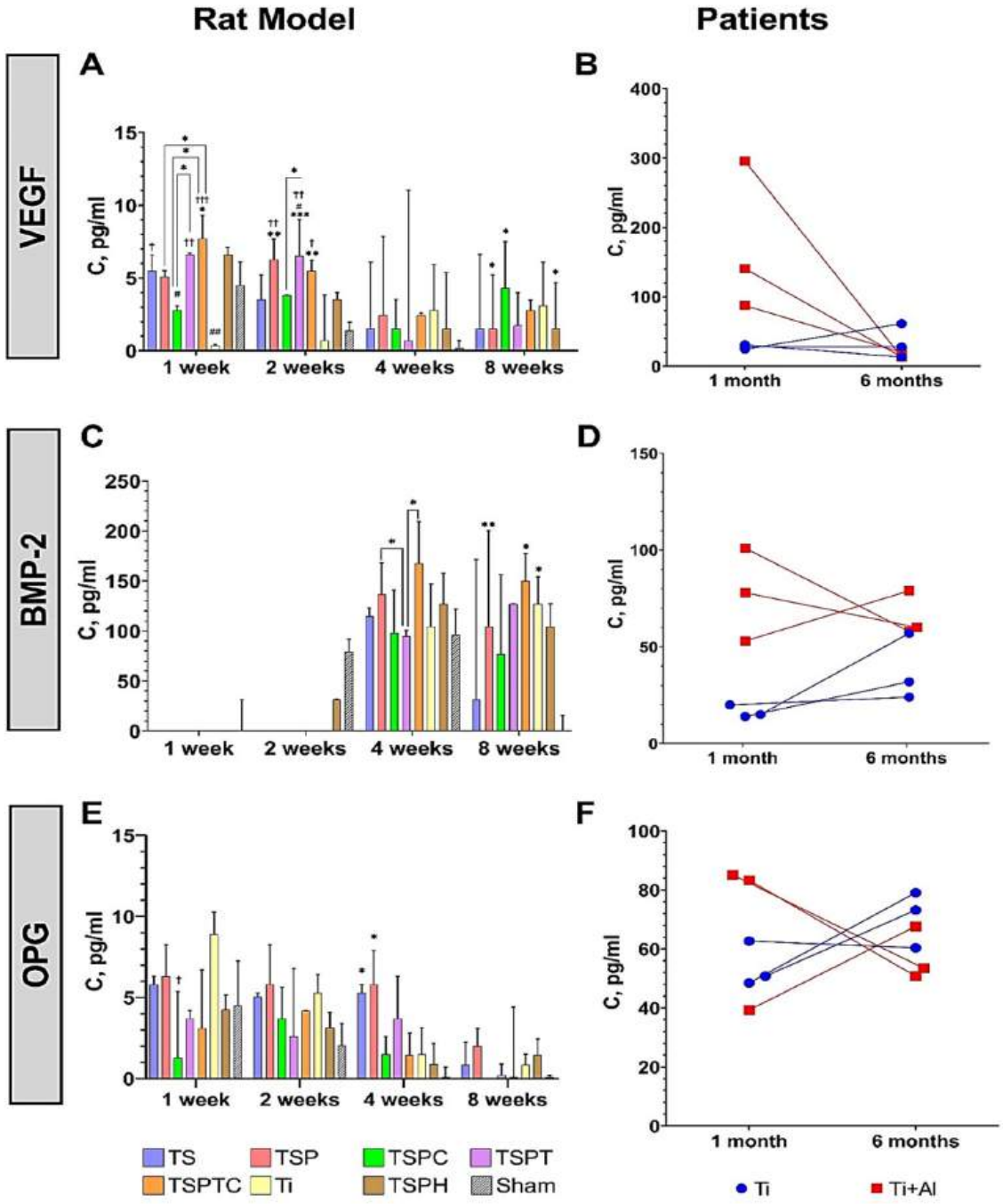

A, C, E –temporal expression profiles of serum VEGF, BMP-2, and OPG in the rat model (n=5 per group/time point). Data are presented as median ± interquartile range (IQR). Statistical significance is indicated as follows: † $p<0.05$, †† $p<0.001$, ††† $p<0.0001$ compared to the uncoated Ti group; # $p<0.05$, ## $p<0.001$ compared to the TSPH (hydroxyapatite) group; * $p<0.05$, ** $p<0.001$, *** $p<0.0001$ compared to the sham control. Brackets with asterisks (*) indicate significant differences between specific experimental pairs identified by post hoc analysis. B, D, F –pilot clinical study showing individual longitudinal trajectories of biomarkers in patients receiving uncoated (Ti, blue circles, n=3) and alumina-coated (Ti+Al, red squares, n=3) implants. Lines connect data points for the same patient to illustrate the directional change from 1 month to 6 months.

Fig. 2. Comparative dynamics of molecular markers serum level in the rat model and pilot clinical study

OPG levels measurements revealed a general downward trend from week 1 to week 8 (Fig. 2E). In a week, the alumina-coated TSPC group demonstrated significantly lower concentrations compared to the uncoated Ti group ($p<0.05$). No other significant inter-group differences were found at this early point. In two weeks, although the median OPG levels in the alumina-coated TSPC and TSPTC groups exhibited a transient increase, no statistically significant inter-group differences were observed. In four weeks, both the TS- and TSP-implanted animals maintained concentrations significantly higher than the sham-operated group ($p<0.05$). No significant inter-group differences were found in eight weeks; moreover, OPG values were minimal across all groups at this time point. Comparing the intra-group dynamics, OPG serum concentrations only in Ti and TS groups showed a significant decline between week 1 and week 8 ($p<0.05$).

The temporal dynamics of molecular markers in the rat model were then compared to the clinical pilot cohort using pattern-matching assessment. As the ELISA measurements from the patients lacked statistical power and consequently revealed no significant differences via inter-group or intra-group comparisons, these results are incorporated into the suggestive pattern-matching assessment described in the paragraph below.

Pattern-Matching Assessment. The pattern-matching analysis compared the molecular trajectories of the pilot clinical cohort with the established preclinical profiles in rat model. VEGF trajectory in patients with alumina-coated implants exhibited a transient upregulation after first month with median value 140.7±208 pg/ml, decreasing by sixth month (13.2±6.5 pg/ml, Fig. 2B). This pattern corresponds with profile of the coated rat group. In contrast, the patients with non-coated implants displayed a relatively stable pattern of VEGF dynamics (27.7±6.4 pg/ml to 27.7±48.1 pg/ml). The dynamics of BMP-2 in patients with alumina-coated implants demonstrated sustained elevation with higher levels after one month (78±48 pg/ml) and maintained after six months (60±21 pg/ml), whereas human Ti group showed a delayed increase (15±6 pg/ml to 32±33 pg/ml, Fig. 2D). OPG-trajectories diverged (Fig. 2F): the uncoated Ti group demonstrated a trend of upregulation (50.8±14.2 to 73.2±18.7 pg/ml), while Ti+Al displayed a stabilizing downward trend (83.3±45.8 to 53.5±16.9 pg/ml).

Immunohistochemical analysis. Histological patterns of VEGFR expression demonstrated marked differences in vascular density and cellular localization across the implant groups at early time points (Fig. 3, A, B).

MVD assessment revealed marked temporal and group-dependent variations throughout the eight-week healing period. In a week, all experimental implant groups demonstrated moderately increased vascularization in comparison to the sham control ($p<0.05$, Table). The maximum value was observed at the two-week point in all samples, with the highest values recorded in the TSPTC and TSPH groups (83.4±7.8 and 80.2±6.1 vessels/mm², respectively; $p<0.05$ vs. sham). After four weeks, the MVD demonstrated a significant decrease in the majority of groups, yet remained elevated in comparison to the sham control group ($p<0.001$). This elevation was particularly pronounced in the TSPT, TSPTC, and Ti groups. In eight weeks, vascular density declined markedly in all samples ($p<0.01$ compared to earlier time points); however, it remained notably higher than that in the sham group for most surface-modified implants.

Immunohistochemical analysis demonstrated time-dependent and surface-specific modulation of BMP-2 expression within peri-implant tissues (Fig. 3 C,D, Table). BMP-2-positive cells were identified among osteoblasts actively lining newly formed trabeculae, endothelial cells of developing capillaries, bone marrow stromal cells, and occasionally within osteocytes embedded in immature bone. Prominent BMP-2 immunostaining was observed in the osteoid matrix adjacent to implant surfaces, colocalizing with areas of new bone deposition. Expression intensity increased significantly across all experimental groups from the first to the fourth week ($p<0.0001$ for intra-group comparisons).

In the second week of the study, the coated titanium groups demonstrated higher levels of BMP-2 than in the first week, exhibiting significant inter-group variations (TS vs. TSPT, $p<0.01$; TS vs. TSPTC, $p<0.0001$; TSP vs. TSPTC, $p<0.05$). The most pronounced cytoplasmic and extracellular BMP-2 reactivity was identified in the fourth week in the groups with coated implants (TSPT, TSPTC, and TSPH), with a strong significant difference compared to the groups with uncoated Ti and sham controls ($p<0.001$). The four-week peak in all groups with coated samples was followed by a gradual decline in the eighth week. Nevertheless, the expression rate for BMP-2 remained significantly higher in TSPT and TSPTC than in uncoated Ti or sham ($p<0.01$). BMP-2 expression was predominantly localized to regions of osteoid formation and early mineralization.

Similarly to previously investigated biomarkers, RANK immunoreactivity exhibited distinct temporal and spatial dynamics across the peri-implant tissues (Fig. 3 E, F; Table). In the early postoperative phase, moderate expression was observed in numerous

mononuclear pre-osteoclast-like cells within the fibrous connective tissue immediately adjacent to implant surfaces. Quantitatively, all groups demonstrated low but substantial intergroup variation, with higher RANK-positive cell counts observed in the groups with alumina-coated implants (TSPC and TSPTC) compared with TS, Ti, and sham ($p<0.05$). By the second week, RANK expression had increased significantly in all experimental groups ($p<0.0001$), reaching maximal values in the TSPT and TSPTC groups, where numerous multinucleated osteoclasts appeared along the newly formed trabeculae. In the fourth week, RANK immunoreactivity remained high, localized along the resorption lacunae at the interface of the maturing bone trabeculae. Similar to the previous periods, noteworthy intra- and intergroup variability persisted ($p<0.0001$). This phase exhibited the highest number of multinucleated RANK-positive osteoclasts, as observed histologically. By the eighth week, there has been a remarkable drop in both the intensity and number of RANK-positive cells across all groups ($p<0.0001$ for most intragroup comparisons). Residual expression was limited to scattered mononuclear cells at the bone-implant interface, with only minor intergroup differences.

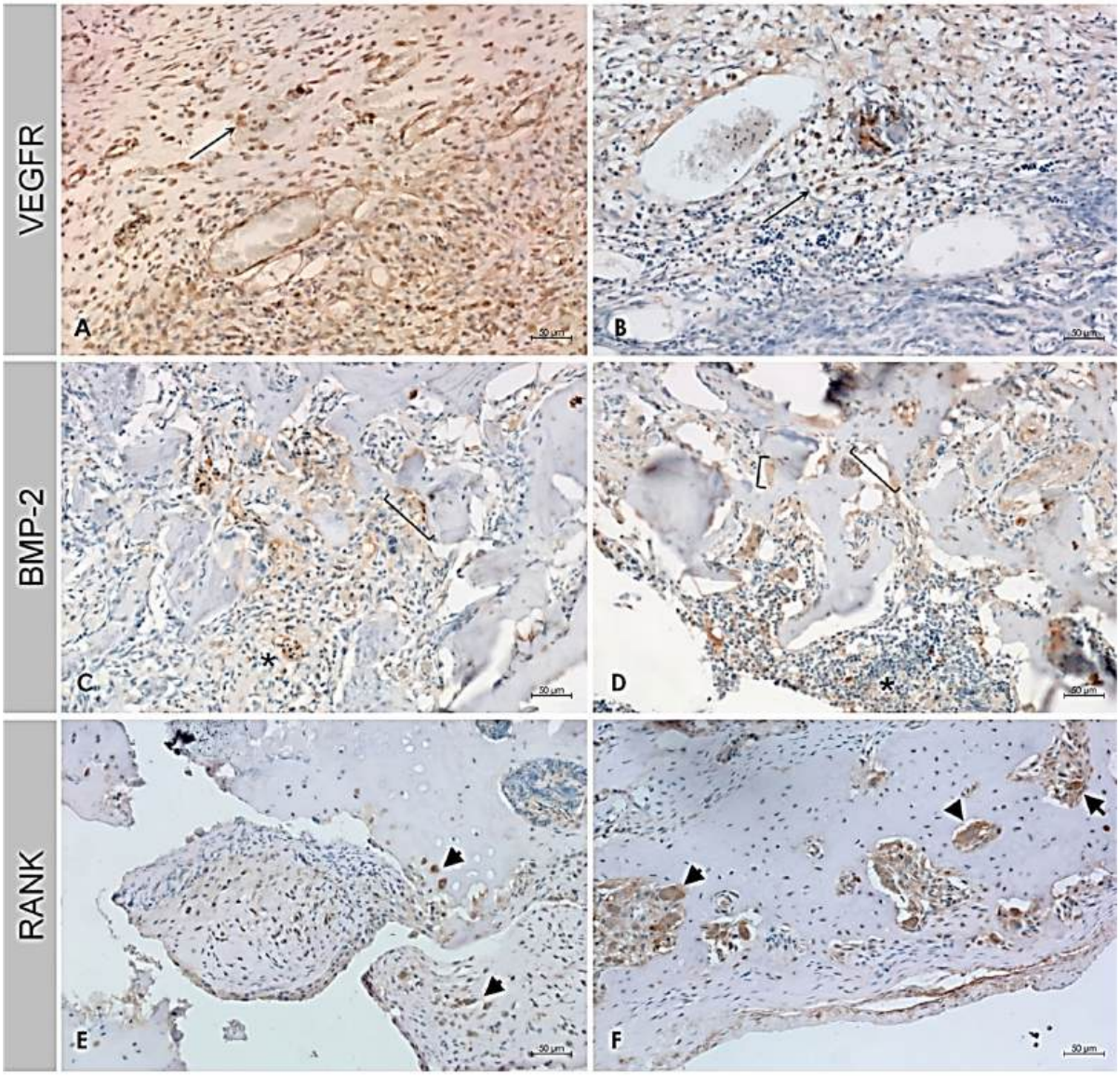

A – numerous small, VEGFR-positive endothelial cells (ECs, arrows) forming capillary loopsin the peri-implant fibrous tissue of TSPTC rat (arrow); B – VEGFR-positive residuals of the granulation tissue with the area of new bone formation around the implant in Ti group in 4 weeks; C – BMP-2 positive areas (brackets) in peri-implant bone and diffusely distributed BMP-2-positive cells in bone marrow (asterisks) of TSPH-contained specimen after 2 weeks; D – Moderate level of BMP-2 expression in newly formed bone around TSPTC implant; E – RANK-positive mesenchymal cells (arrowheads) in peri-implant area (TSP-group, 2 weeks); F – RANK-positive osteoclasts (arrowheads) in lacunae of the newly formed bone (TSPTC-group, 4 weeks).

Fig. 3. Representative patterns of VEGFR (A and B), BMP-2 (C and D), and RANK (E and F) immunostaining in peri-implant tissues. Immunoperoxydase method, ×400

Microvascular density (MVD), BMP-2, and RANK expression in peri-implant tissue of experimental animals, mean value ± SD

Observation period	TS	TSP	TSPC	TSPT	TSPTC	Ti	TSPH	Sham
				MVD, vessels/mm^2				
Week 1	35.3±2.45^{a}	34.22±1.46^{a}	36.52±2.74^{a}	29.8±2.53	35.28±2.06^{a}	32.68±3.07	30.42±1.93	28.12±1.93
Week 2	72.8±4.19	73.5±3.89	79.12±4.06	82.7±5.42	83.36±4.32^{a}	72.78±2.79	80.18±2.81^{a}	68.88±3.49
Week 4	56.42±3.40^{a}	51.6±3.61^{a}	52.44±2.32^{a,b}	57.8±2.59^{a}	54.24±4.52^{a}	59.82±2.45^{a,c}	49.84±3.62^{a}	26.6±4.0
Week 8	28.32 ±2.34^{a,b,c}	24.9±2.02^{a,b}	21.82±1.81^{b}	24.7±1.47^{a,b,c}	25.64±1.11^{a,b,c}	36.18±1.60^{a,c}	19.92±0.92	19.4±1.27
				BMP-2 positive cells/ROI				
Week 1	13.6±1.14	13. ±2.39	15.8±2.49	17.6±1.14	19.2±3.27	12.6±1.52	18.2±1.92	17.2±1.92
Week 2	25.6±2.97^{a}	27.6±3.05	33.6±2.70^{b}	35.2±3.77^{b}	38.4±2.88^{b}	20.4±3.51^{a,c}	32.0±6.20	33.2±3.42
Week 4	48.0±4.00^{a,c}	53.0±3.41^{c}	55.0±4.74^{b,c}	61.8±4.76^{b}	62.0±3.00^{b}	47.4±4.62^{a,c}	65.8±4.15	58.4±6.19
Week 8	31.2±4.21^{c}	27.6±4.51^{c}	35.6±5.03^{a,b,c}	37.8±6.53^{b}	40.2±4.02^{a,b}	25.0±1.58^{c}	43.4±2.70^{a}	27.8±2.86
				RANK-positive cells/ROI				
Week 1	23.0±3.16^{b,c}	24.0±5.15	31.0±3.39^{a}	30.8±3.19^{a}	34.0±2.00^{a}	29.2±1.92^{a}	29.4±2.97^{a}	20.8±2.39
Week 2	32.0±3.16	37.8±7.98^{a}	40.4±2.07^{a,c}	40.8±2.28^{a,b,c}	43.6±3.85^{a,b,c}	34.6±2.97	34.0±2.65	30.2±1.92
Week 4	18.2±3.90	24.4±4.62^{a}	26.4±3.05^{a}	28.0±3.16^{a,c}	30.0±2.00^{a,b,c}	23.4±2.70	20.8±2.39	17.8±2.39
Week 8	15.4±1.14^{a}	16.6±1.14	17.0±1.58	18.2±1.92^{a}	17.4±2.41	15.0±1.58	13.6±1.14	12.2±1.48

Notes: Superscript letters (a,b,c) indicate statistically significant differences between groups at the same time point ($p<0.05$): a – sham control; b – untreated titanium (Ti-group); c – reference group with HAp-coated implants.

The process of osseointegration is contingent upon the rapid development of neovascularization [1]. The investigation revealed that alumina-based coatings effectively stimulated an accelerated angiogenic phase, evidenced by a robust one-week peak of VEGF expression in rats that significantly exceeded uncoated titanium. This finding was qualitatively mirrored by clinical observations, where the Ti+Al group exhibited an elevated systemic VEGF trend during the initial month in comparison to the Ti group. The subsequent decline in VEGF in coated groups across both models indicates a well-regulated and transient response, marking the timely completion of the early vascular phase and efficient transition to bone formation – an essential kinetic profile for optimal healing [3, 4]. Conversely, minimal early VEGF activity in uncoated implants suggests delayed vascular stimulation.

This systemic acceleration was supported by the local findings. MVD, as determined by VEGFR immunodetection, reached its peak in the second week, confirming the period of intensive local vascular support. Of particular significance is the sustained vascularization observed around alumina- and hydroxyapatite-coated implants (TSPTC and TSPH) at later stages, despite the systemic decline in VEGF. This finding suggests the presence of prolonged, localized angiogenic activity promoted by surface bioactivation. This phenomenon has heretofore been documented as an augmented process of osseointegration [5, 6, 15].

The accelerated angiogenic phase is observed to immediately precede and may even overlap with the accelerated osteoinduction phase. The human data were particularly revealing BMP-2 levels upregulation in the Ti+Al group in the first month compared to the Ti group, indicating that the alumina-based coating not only enhances angiogenesis but also advances the systemic induction of osteogenic signaling. BMP-2, the most potent osteoinductive growth factor, has been demonstrated to drive migration, proliferation, and osteoblastic differentiation of osteoprogenitor cells [6,13]. The coated groups exhibited a delayed sharp rise leading to a peak in four weeks, followed by a period of stabilization, thereby substantiating the hypothesis

that this synchronized and intense signaling profile compresses the overall duration of the early regenerative phase and demonstrates the expedited shift into the sustained new bone formation and remodeling phase. This systemic profile was corroborated by local IHC findings: in rats, the definitive systemic rise of BMP-2 at week 4 aligned precisely with histological peaks of BMP-2 in osteoblasts and osteoid, confirming synchronized local and systemic osteoinductive signaling. While serum BMP-2 levels converged across the coated groups in the four-week peak (reflecting the overall remodeling rate), the local intensity remained higher around alumina-coated surfaces (reflecting coating-specific enhancement).

The regulation of early bone remodeling through the OPG pathway revealed a nuanced, primarily local effect. In rats, uncoated titanium (Ti) generated a strong immediate protective anti-resorptive OPG peak, likely reflecting a response to the bare untreated surface. Conversely, alumina-based coatings have been shown to significantly attenuate this peak, suggesting that less anti-resorptive signaling is required. This attenuation can be attributed to the coating's inherent biocompatibility and its rapid promotion of osteogenesis, potentially representing a smoother remodeling process that warrants further investigation [17]. However, in humans, coating-related differences in systemic OPG levels did not achieve statistical significance, indicating that alumina coatings primarily accelerate bone formation rather than fundamentally altering systemic bone resorption during the early healing phase. This finding is consistent with others *in vivo* surface modification studies [24].

To enhance comprehension of local remodeling events, RANK immunostaining was appraised. The initial upregulation of RANK in groups coated with alumina has been demonstrated to result in accelerated osteoclast differentiation and activation at the bone-implant interface. The controlled osteoclastic activity facilitates matrix turnover and creates space for new bone deposition, thereby supporting more efficient integration. The peak in week 4 corresponded to maximal trabecular remodeling, while the decline by week 8, particularly in coated implants, indicated a shift towards remodeling equilibrium and tissue maturation. These findings indicate that alumina-based surfaces do not merely enhance formation but also refine the dynamics of resorption, thereby promoting balanced, accelerated bone renewal and superior integration outcomes in comparison with uncoated titanium [25].

Despite the compelling molecular parallelism established between the rat model and human patients, several limitations inherent to translational osseointegration studies must be considered. The primary limitation in the clinical component is the small human sample size (n=6). Recognizing that this low power of the study introduces a high risk of failing to detect a true biological effect and renders the results highly sensitive to outliers, we adopted a configurational pattern-matching approach to evaluate directional consistency rather than statistical magnitude. Nevertheless, clinical findings should be interpreted as distinct pilot evidence requiring validation in larger cohorts. Furthermore, the allometric disparity in bone metabolism; the rat's significantly faster healing rate (consolidation in 5-6 weeks) necessitates the use of biologically equivalent phases rather than chronological time points [26]. Additionally, the experimental model utilized simple intramedullary pins, which cannot fully replicate the complex biomechanical loading and stress shielding experienced by large-scale human hip prostheses. Finally, while the molecular markers for angiogenesis (VEGF) and osteoinduction (BMP-2) showed certain translational parallelism, the divergence in systemic OPG dynamics suggests that systemic regulation of bone remodeling is highly species-specific and may not be accurately modeled by the rodent system, as was reported previously [27]. Consequently, conclusions regarding long-term stability and comprehensive biomechanical integration must remain cautious pending further long-term clinical data.

The present study provides compelling molecular and immunohistochemical evidence that alumina-based titanium coatings (TSPTC, Ti+Al) induce an accelerated and highly regulated early regenerative response that is critical for successful osseointegration. A central finding is the direct translational link established for key pro-regenerative markers. While statistical significance was not achieved in the human pilot cohort, the suggestive pattern of early VEGF upregulation followed by sustained BMP-2 elevation observed in the rat model was qualitatively replicated in human patients via pattern-matching analysis. The consistency observed between the preclinical and pilot clinical findings suggests the translational potential of the investigated biomarkers and the pattern-matching methodology for guiding implant assessment. While the rat model provided initial data, future studies should focus on refining these patterns in larger animal models that more closely mimic the human physiological and biomechanical environment, thereby enhancing the predictive power of the molecular configuration prior to large-scale human trials [26].

CONCLUSIONS

1. Alumina-coated titanium implants (TSPTC, Ti+Al) have been shown to induce a molecular signature that is characterized by a rapid, synchronized

cascade from neoangiogenesis to osteoinduction. The sequence under consideration involves an early systemic VEGF peak and a local peak of VEGFR expression in the first week of implantation, which is immediately followed by a synchronized systemic and local peak of BMP-2 in the fourth week.

2. This sequence indicates a significantly accelerated and more efficient initiation of the healing process compared to uncoated titanium (Ti). This acceleration, evidenced by the BMP-2 concentration in TSPTC group versus Ti group at week 4, achieved high statistical significance ($p<0.001$).

3. The alumina-based coating demonstrated an enhanced osteoconductive capacity by actively orchestrating a balanced remodeling process. The local IHC evidence for the expression of RANK and sustained neoangiogenesis was indicative of the fact that the alumina-based coating promoted accelerated osteoblast activity and controlled bone resorption activity, which peaked in the fourth week. These effects result in rapid matrix turnover and early stabilization of the peri-implant bone.

4. Notwithstanding the molecular parallels between the experimental model on rats and post-surgical follow-up of the patients with hip replacement observed for pro-regenerative markers (VEGF, BMP-2), the interpretation of findings must be conducted with caution, given the inherent translational constraints. These constraints encompass the limited human sample size (n=6, with elevated statistical risk) and the discrepancy in allometric and biomechanical characteristics between the rat model and human prostheses, and the observed divergence in systemic OPG dynamics, suggesting species-specific bone remodeling regulation.

Contributors:

Bondarenko O.O. – conceptualization, methodology, investigation, formal analysis, visualization, validation, writing – original draft;

Lievykh A.E. – conceptualization, methodology, investigation, formal analysis;

Bondarenko N.S. – investigation, formal analysis, validation, data curation;

Bozhko A.G. – conceptualization, methodology, investigation;

Loskutov O.Ye. – validation, project administration, supervision, data curation, writing – review &editing;

Shponka I.S. – validation, project administration, supervision, resources, data curation, writing – review &editing;

Funding. This study was a part of the research project "Molecular-genetic and morphological features of reparative bone regeneration using functional-protective coatings of implant materials" with a governmental funding, statenumberof registration 0119U101119.

Conflict of interests. The authors declare no conflict of interest.

REFERENCES

1. Helaehil JV, Huang B, Bartolo P, Santamaria-Jr M, Caetano GF. Bone regeneration: The influence of composite HA/TCP scaffolds and electrical stimulation on TGF/BMP and RANK/RANKL/OPG pathways. Injury. 2025;56(2):112158.
doi: https://doi.org/10.1016/j.injury.2025.112158

2. Tan B, Liu X, Chen S, et al. An injectable nano-hydroxyapatite-incorporated hydrogel with sustained release of Notoginsenoside R1 enhances bone regeneration by promoting angiogenesis through Notch1/Akt signaling. J Adv Res. 2025 May 13:S2090-1232(25)00343-1.
doi: https://doi.org/10.1016/j.jare.2025.05.025

3. Cao L, Wang J, Hou J, Xing W, Liu C. Vascularization and bone regeneration in a critical sized defect using 2-N,6-O-sulfated chitosan nanoparticles incorporating BMP-2. Biomaterials. 2014;35(2):684-98.
doi: https://doi.org/10.1016/j.biomaterials.2013.10.005

4. Ramazanoglu M, Lutz R, Rusche P, et al. Bone response to biomimetic implants delivering BMP-2 and VEGF: an immunohistochemical study. J Craniomaxillofac Surg. 2013;41(8):826-35.
doi: https://doi.org/10.1016/j.jcms.2013.01.037

5. Verisqa F, Park JH, Mandakhbayar N, et al. In Vivo Osteogenic and Angiogenic Properties of a 3D-Printed Isosorbide-Based Gyroid Scaffold Manufactured via Digital Light Processing. Biomedicines. 2024;12(3):609.
doi: https://doi.org/10.3390/biomedicines12030609

6. Steiner D, Reinhardt L, Fischer L, et al. Impact of Endothelial Progenitor Cells in the Vascularization of Osteogenic Scaffolds. Cells. 2022;11(6):926.
doi: https://doi.org/10.3390/cells11060926

7. Astudillo Potes MD, Mitra I, Hanson K, et al. Biodegradable poly(caprolactone fumarate) 3D printed scaffolds for segmental bone defects within the Masquelet technique. J Orthop Res. 2024;42(9):1974-83.
doi: https://doi.org/10.1002/jor.25839

8. Al Qabbani A, Rani KGA, AlKawas S, et al. Evaluation of the osteogenic potential of demineralized and decellularized bovine bone granules following implantation in rat calvaria critical-size defect model. PLoS One. 2023;18(12):e0294291.
doi: https://doi.org/10.1371/journal.pone.0294291

9. Basal O, Ozmen O, Deliormanli AM. Effect of polycaprolactone scaffolds containing different weights of graphene on healing in large osteochondral defect model. J Biomater Sci Polym Ed. 2022;33(9):1123-39.
doi: https://doi.org/10.1080/09205063.2022.2042035

10. Dang L, Zhu J, Song C. The effect of topical administration of simvastatin on entochondrostosis and intramembranous ossification: An animal experiment. J Orthop Translat. 2021;28:1-9.
doi: https://doi.org/10.1016/j.jot.2020.11.009

11. Cen C, Zhang Y, Cao Y, et al. Construction of a 3D Degradable PLLA/β-TCP/CS Scaffold for Establishing an Induced Membrane Inspired by the Modified Single-Stage Masquelet Technique. ACS Biomater Sci Eng. 2025;11(3):1629-45.
doi: https://doi.org/10.1021/acsbiomaterials.4c01849

12. Yiğit U, Kırzıoğlu FY, Özmen Ö. Effects of low dose doxycycline and caffeic acid phenethyl ester on sclerostin and bone morphogenic protein-2 expressions in experimental periodontitis. Biotech Histochem. 2022;97(8):567-75.
doi: https://doi.org/10.1080/10520295.2022.2036370

13. Gao J, Zhang G, Xu K, et al. Bone marrow mesenchymal stem cells improve bone erosion in collagen-induced arthritis by inhibiting osteoclasia-related factors and differentiating into chondrocytes. Stem Cell Res Ther. 2020;11(1):171.
doi: https://doi.org/10.1186/s13287-020-01684-w

14. Fawaz A, Mohammed MM, Ismail A, Rani KGA, Samsudin AR. The influence of simvastatin on osteoblast functionality in the presence of titanium dioxide particles In-vitro. Arch Oral Biol. 2024;167:106065.
doi: https://doi.org/10.1016/j.archoralbio.2024.106065

15. Fiorin LG, Matheus HR, Ervolino E, et al. Tamoxifen improves homeostasis in the peri-implant bone remodeling of osseointegrated titanium implants. J Periodontal Res. 2022;57(4):880-90.
doi: https://doi.org/10.1111/jre.13026

16. Ke Re Mu ALM, Abulikemu M, Liang Z, Abulikemu A, Tuxun A. Anti-Infection Efficacy, Osteogenesis Potential, and Biocompatibility of 3D Printed PLGA/Nano-Hydroxyapatite Porous Scaffolds Grafted with Vancomycin/DOPA/rhBMP-2 in Infected Rabbit Bone Defects. Int J Nanomedicine. 2025;20:6399-421.
doi: https://doi.org/10.2147/IJN.S514978

17. Kim JE, Takanche JS, Jang S, Yi HK. Mussel adhesive protein blended with gelatin loaded into nanotube titanium dental implants enhances osseointegration. Drug Deliv Transl Res. 2021;11(3):956-65.
doi: https://doi.org/10.1007/s13346-020-00807-3

18. Durand M, Oger M, Nikovics K, et al. Influence of the Immune Microenvironment Provided by Implanted Biomaterials on the Biological Properties of Masquelet-Induced Membranes in Rats: Metakaolin as an Alternative Spacer. Biomedicines. 2022;10(12):3017.
doi: https://doi.org/10.3390/biomedicines10123017

19. Loskutov O, Shponka I, Bondarenko O, Bondarenko N, Bozhko A. Histological and histochemical assessment of short-term events in peri-implant bone for osteoinductivity evaluation of functional-protective implant coatings. Medicni perspektivi 2021;26(3):4-10.
doi: https://doi.org/10.26641/2307-0404.2021.3.241875

20. Bondarenko OO, Bozhko AH, Skoryk MA, Bondarenko NS, Shponka IS, Loskutov OY. Peri-implant osteogenesis on alumina-coated titanium implants in rat femur: morphological and elemental analysis of implant surfaces. Pathologia. 2024;21(2):132-40.
doi: https://doi.org/10.14739/2310-1237.2024.2.306822

21. Sanderson T, Wild G, Cull AM, Marston J, Zardin G. Immunohistochemical and immunofluorescent techniques. In: Suvarna SK, Layton C, Bancroft JD, editors. Bancroft's Theory and Practice of Histological Techniques. 8th ed. Elsevier; 2019. p. 337-94.
doi: https://doi.org/10.1016/B978-0-7020-6864-5.00019-0

22. Hak T, Dul J. Pattern matching. In: Mills AJ, Durepos G, Wiebe E, editors. Encyclopedia of case study research. Thousand Oaks (CA): SAGE; 2010. p. 664-6.

23. Claes L, Recknagel S, Ignatius A. Fracture healing under healthy and inflammatory conditions. Nat Rev Rheumatol. 2012 Jan 31;8(3):133-43.
doi: https://doi.org/10.1038/nrrheum.2012.1

24. Camilo CC, Silveira CAE, Faeda RS, de Almeida Rollo JMD, Purquerio BM, Fortulan CA. Bone response to porous alumina implants coated with bioactive materials, observed using different characterization techniques. J Appl Biomater Funct Mater. 2017;15(3):e223-e235.
doi: https://doi.org/10.5301/jabfm.5000347

25. Lukaszewska-Kuska M, Wirstlein P, Majchrowski R, Dorocka-Bobkowska B. The effects of titanium topography and chemical composition on human osteoblast cell. Physiol Res. 2021;70(3):413-23.
doi: https://doi.org/10.33549/physiolres.934582

26. Zeiter S, Koschitzki K, Alini M, Jakob F, Rudert M, Herrmann M. Evaluation of Preclinical Models for the Testing of Bone Tissue-Engineered Constructs. Tissue Eng Part C Methods. 2020;26(2):107-17.
doi: https://doi.org/10.1089/ten.TEC.2019.0213

27. Blanc-Sylvestre N, Bouchard P, Chaussain C, Bardet C. Pre-Clinical Models in Implant Dentistry: Past, Present, Future. Biomedicines. 2021;9(11):1538.
doi: https://doi.org/10.3390/biomedicines9111538

Стаття надійшла до редакції 20.10.2025;
затверджена до публікації 14.11.2025